

Exact radial free vibration frequencies of a thick-walled sphere made of an isotropic and homogeneous material – A case study with a carbon nanofiller reinforced aluminum hollow sphere

Vebil Yıldırım

Online Publication Date: 17 July 2018

URL: <http://dx.doi.org/10.17515/resm2017.24me0608>

DOI: <http://dx.doi.org/10.17515/resm2017.24me0608>

Journal Abbreviation: *Res. Eng. Struct. Mat.*

To cite this article

Yıldırım V. Exact radial free vibration frequencies of a thick-walled sphere made of an isotropic and homogeneous material – A case study with a carbon nanofiller reinforced aluminum hollow sphere. *Res. Eng. Struct. Mat.*, 2019; 5(1): 13-32.

Disclaimer

All the opinions and statements expressed in the papers are on the responsibility of author(s) and are not to be regarded as those of the journal of Research on Engineering Structures and Materials (RESM) organization or related parties. The publishers make no warranty, explicit or implied, or make any representation with respect to the contents of any article will be complete or accurate or up to date. The accuracy of any instructions, equations, or other information should be independently verified. The publisher and related parties shall not be liable for any loss, actions, claims, proceedings, demand or costs or damages whatsoever or howsoever caused arising directly or indirectly in connection with use of the information given in the journal or related means.



Research Article

Exact radial free vibration frequencies of a thick-walled sphere made of an isotropic and homogeneous material – A case study with a carbon nanofiller reinforced aluminum hollow sphere

Vebil Yıldırım^a

Çukurova University Department of Mechanical Engineering, Adana, Turkey

Article Info

Article history:

Received 08 June 2017

Revised 19 June 2018

Accepted 17 July 2018

Keywords:

Exact free vibration,
Natural frequency,
Thick-walled sphere,
Spherical Bessel's,
Metal-matrix
composites (MMCs)

Abstract

In this study exact free vibration analysis is performed for thick-walled hollow spheres made of an isotropic and homogeneous linear elastic material. Equation of motion in terms of Lamé constants is derived from the field equations of elasticity, and then solved analytically with the help of spherical Bessel's functions. This existing solution technique is extended to several boundary conditions. For each classical boundary condition, the characteristic free vibration equation is presented in closed forms. After verifying the present results with the available literature, variation of the dimensionless natural frequencies with respect to the boundary conditions and the sphere aspect ratio (outer radius/inner radius) are examined. To show the direct use of the present results, some of which are originals, a case study for a metal-matrix composite is originally studied. This composite material is formed by a perfect dispersion of either single-walled carbon-nanotubes (SWCNT) or multi-walled carbon-nanotubes (MWCNT) within an Aluminum (AL) metal matrix so that the resulting composite is still to have both isotropy and homogeneity properties. Elastic properties of the composite are computed by using the simple mixture rule and Halpin-Tsai equations.

© 2018 MIM Research Group. All rights reserved

1. Introduction

Vibration of thick-walled spheres is of great importance in many engineering applications. Pioneering studies date back 1880s [1-2]. As easily guessed, in the first works in this realm, spheres are assumed to be made of traditional materials having both isotropy and homogeneity properties [3-9]. Among those, Sato and Usami [3-4] presented a basic study on the oscillation of homogeneous elastic sphere. Shah et al. [5-6] examined analytically and numerically the elastic waves in a hollow sphere based on the three dimensional shell theory. Seide [7] derived the frequency equation in radial direction for hollow thin spheres. Fixed boundary conditions for the free vibration analysis of elastic spheres were studied by Scaffbuch et. al. [8]. Gosh and Agrawal [9] worked analytically on the free and forced radial vibrations of spheres by employing Bessel's functions as in the present study. Explicit expressions were presented for the natural frequencies and dynamic stresses for various time-varying internal pressures in Gosh and Agrawal' work [9]. Abbas [10] presented an analytical solution for the free vibration of a thermo-elastic hollow sphere.

*Corresponding author: vebil@cu.edu.tr

^aorcid.org/ 0000-0001-9955-8423

DOI: <http://dx.doi.org/10.17515/resm2017.24me0608>

Res. Eng. Struct. Mat. Vol. 5 Iss. 1 (2019) 13-32

Sharma and Sharma [11] and Sharma [12] also studied free vibration of thermoelastic solid and hollow spheres, respectively.

Numerous studies have been continued up to now by employing advanced materials with thermal, magnetic and whatnot effects. Among them, vibration analysis of spheres made of anisotropic materials occupy a great deal of space in the open literature [13-29]. Eason [14] firstly examined the pure radial free vibration of transversely isotropic spheres. Grigorenko and Kilina [18] handled 2-D and 3-D formulation of the problem at stake. Jiang et al. [20] investigated free vibration of layered hollow spheres using three-dimensional elasticity. After Eason [14], Stavsky and Greenberg [26], Ding and Wang [27], and Keles [29] have addressed purely radial free vibrations for anisotropic spheres. Chen et al. [30] dealt with free vibrations of a piezoceramic fluid-filled hollow sphere. Chiroiu and Munteanu [31] omitted fluid effects on the free vibration of a piezoceramic sphere. Lately free vibrations of spheres made of functionally graded materials have been gained an attention [32-38].

This study deals with only purely radial free vibration of hollow spheres made of both isotropic and homogeneous material. The principal aim of the present study is to present a detailed source for engineers and young scientists. To this end, as a very fundamental problem, the exact free vibration analysis of a thick-walled hollow sphere with the inner radius a and the outer radius b have been reconsidered (Fig. 1) [9]. The ratio (b/a) is defined as an aspect ratio of the sphere. When doing this, the solution method proposed by Gosh and Agarwal [9] are step-by-step extended to additional boundary conditions. The effects of the aspect ratio on the exact dimensionless radial natural frequencies are also examined. These results, some of which are original, may also be served as a comparison means. Those natural frequencies may also be used directly to study the exact dynamic response of such structures as in References [9, 36].

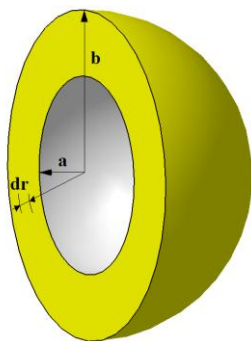


Fig. 1 Geometry of a sphere

Besides, to consider a kind of emerging state of the art technological materials [39-41], a very simple example, which may be solved by direct application of the present formulation to the free vibration of a hollow sphere made of a carbon nanotube reinforced metal, is to be examined.

It is also worth noting that the present formulation may easily be extended to the radial free vibration of spheres, cylinders, or disks made of either ordinary orthotropic or functionally graded materials as in References [36, 38, 42-43].

2. Formulation

The strain-displacement relations under axisymmetric conditions are given in spherical coordinates, (r, θ, ϕ) , by (Fig. 1)

$$\begin{aligned}\varepsilon_r &= \frac{du_r}{dr} \\ \varepsilon_\theta &= \varepsilon_\phi = \frac{u_r}{r}\end{aligned}\tag{1}$$

where ε_r is the radial unit strain, ε_θ is the tangential unit strain and u_r is the radial displacement. Denoting the radial stress by σ_r , and the hoop stress by σ_θ , Hooke's law for spheres is written as follows

$$\begin{aligned}\sigma_r &= C_{11} \varepsilon_r + C_{12} \varepsilon_\theta \\ \sigma_\theta &= C_{21} \varepsilon_r + C_{22} \varepsilon_\theta\end{aligned}\tag{2}$$

where the stiffness terms may be defined by Lamé's constants for an isotropic and homogeneous linear elastic material as

$$\begin{aligned}C_{11} &= \lambda + 2\mu \quad ; C_{12} = 2\lambda \\ C_{21} &= \lambda \quad ; C_{22} = 2\lambda + 2\mu\end{aligned}\tag{3}$$

Representing Poisson's ratio by ν , and elasticity modulus by E , Lamé's constants are defined as

$$\begin{aligned}\lambda &= \frac{\nu E}{(1 + \nu)(1 - 2\nu)} \\ \mu &= \frac{E}{2(1 + \nu)}\end{aligned}\tag{4}$$

In the absence of the body forces, equation of motion in the radial direction is given by

$$\frac{1}{r^2} \frac{\partial}{\partial r} (r^2 \sigma_r) - \frac{2\sigma_\theta}{r} = \frac{\partial \sigma_r}{\partial r} + \frac{2(\sigma_r - \sigma_\theta)}{r} = \rho \frac{\partial^2 u_r}{\partial t^2}\tag{5}$$

where ρ is the material density and t is the time. Substituting strain-displacement relations and Hooke's law in the equation of motion, and taking the first derivative of the radial stress with respect to the radial coordinate we obtain

$$\frac{\partial^2 u_r}{\partial r^2} + \frac{2}{r} \frac{\partial u_r}{\partial r} - \frac{2}{r^2} u_r = \frac{\rho}{C_{11}} \frac{\partial^2 u_r}{\partial t^2}\tag{6}$$

By assuming the following harmonic motion with an angular velocity ω (rad/s)

$$u_r(r,t) = u_r^*(r) e^{i\omega t} \tag{7}$$

Eq. (6) turns into Bessel's differential equations as follows [44-47]

$$\left(-\frac{2}{r^2} + \frac{\rho}{\lambda + 2\mu} \omega^2\right) u_r^* + \frac{2}{r} \frac{du_r^*}{dr} + \frac{d^2 u_r^*}{dr^2} = 0 \tag{8}$$

The solutions to this equation will be in terms of the first and second kinds spherical Bessel's functions, $j_n(x)$ and $y_n(x)$ [44-47].

$$u_r^*(r) = C_1 j_1(r\Omega) + C_2 y_1(r\Omega) \tag{9}$$

where

$$\Omega^2 = \frac{\rho}{\lambda + 2\mu} \omega^2 \tag{10}$$

The first derivative of the solution of the radial displacement, u_r^* , and the radial stress, σ_r^* , may be obtained in terms of integration constants, C_1 and C_2 , as follows [44-47]

$$\begin{aligned} \frac{du_r^*}{dr} = & C_1 \Omega \left(\frac{1}{2} (j_0(r\Omega) - j_2(r\Omega)) - \frac{j_1(r\Omega)}{2r\Omega} \right) \\ & + C_2 \Omega \left(\frac{1}{2} (y_0(r\Omega) - y_2(r\Omega)) - \frac{y_1(r\Omega)}{2r\Omega} \right) \end{aligned} \tag{11}$$

$$\begin{aligned} \sigma_r^* = & \frac{1}{r^3 \Omega^2} \left(\sin(r\Omega) (-4C_1 \mu + C_1 r^2 \Omega^2 (\lambda + 2\mu) + 4C_2 \mu r \Omega) \right. \\ & \left. + \cos(r\Omega) (4C_1 \mu r \Omega + 4C_2 \mu - C_2 r^2 \Omega^2 (\lambda + 2\mu)) \right) \end{aligned}$$

Boundary conditions considered in this study is presented in Table 1. If one applies these constraints, the following may be obtained for free-free ends.

$$\mathbf{A}_{Free-Free} \begin{Bmatrix} C_1 \\ C_2 \end{Bmatrix} = \begin{bmatrix} a_{11} & a_{12} \\ a_{21} & a_{22} \end{bmatrix} \begin{Bmatrix} C_1 \\ C_2 \end{Bmatrix} = \begin{Bmatrix} 0 \\ 0 \end{Bmatrix} \tag{12}$$

In the above

$$\begin{aligned} a_{11} = & \frac{a^2 \lambda \sin(a\Omega) \Omega^2 + 2a^2 \mu \sin(a\Omega) \Omega^2 + 4a\mu \cos(a\Omega) \Omega - 4\mu \sin(a\Omega)}{a^3 \Omega^2} \\ a_{12} = & \frac{-a^2 \lambda \cos(a\Omega) \Omega^2 - 2a^2 \mu \cos(a\Omega) \Omega^2 + 4a\mu \sin(a\Omega) \Omega + 4\mu \cos(a\Omega)}{a^3 \Omega^2} \\ a_{21} = & \frac{b^2 \lambda \sin(b\Omega) \Omega^2 + 2b^2 \mu \sin(b\Omega) \Omega^2 + 4b\mu \cos(b\Omega) \Omega - 4\mu \sin(b\Omega)}{b^3 \Omega^2} \\ a_{22} = & \frac{-b^2 \lambda \cos(b\Omega) \Omega^2 - 2b^2 \mu \cos(b\Omega) \Omega^2 + 4b\mu \sin(b\Omega) \Omega + 4\mu \cos(b\Omega)}{b^3 \Omega^2} \end{aligned} \tag{13}$$

For non-trivial natural frequencies, the determinant of $\mathbf{A}_{Free-Free}$ must be equal to zero. This is called characteristic equation. For boundary conditions given in Table 1, characteristic equations for different boundary conditions are found as follows

$$\begin{aligned}
 |\mathbf{A}_{Free-Free}| &= 4\mu\Omega(a-b)\cos(\Omega(a-b))(ab\Omega^2(\lambda+2\mu)+4\mu) \\
 &\quad - \sin(\Omega(a-b))(a^2b^2\Omega^4(\lambda+2\mu)^2 \\
 &\quad - 4\mu\Omega^2(\lambda(a^2+b^2)+2\mu(a-b)^2)+16\mu^2) = 0
 \end{aligned}
 \tag{14a}$$

$$\begin{aligned}
 |\mathbf{A}_{Fixed-Free}| &= j_1(a\Omega)(4b\mu\Omega\sin(b\Omega) - \cos(b\Omega)(b^2\Omega^2(\lambda+2\mu) - 4\mu)) \\
 &\quad + y_1(a\Omega)(-\sin(b\Omega)(b^2\Omega^2(\lambda+2\mu) - 4\mu) \\
 &\quad - 4b\mu\Omega\cos(b\Omega)) = 0
 \end{aligned}$$

$$\begin{aligned}
 |\mathbf{A}_{Free-Fixed}| &= j_1(b\Omega)(\cos(a\Omega)(a^2\Omega^2(\lambda+2\mu) - 4\mu) - 4a\mu\Omega\sin(a\Omega)) \\
 &\quad + y_1(b\Omega)(\sin(a\Omega)(a^2\Omega^2(\lambda+2\mu) - 4\mu) \\
 &\quad + 4a\mu\Omega\cos(a\Omega)) = 0
 \end{aligned}
 \tag{14b}$$

$$|\mathbf{A}_{Fixed-Fixed}| = j_1(a\Omega)y_1(b\Omega) - y_1(a\Omega)j_1(b\Omega) = 0$$

Table 1 Boundary conditions considered in this study.

	Free-Free	Fixed-Free	Fixed-Fixed	Free-Fixed
at ($r = a$)	$\sigma_r^*(a) = 0$	$u_r^*(a) = 0$	$u_r^*(a) = 0$	$\sigma_r^*(a) = 0$
at ($r = b$)	$\sigma_r^*(b) = 0$	$\sigma_r^*(b) = 0$	$u_r^*(b) = 0$	$u_r^*(b) = 0$

Defining the dimensionless natural frequency as follows

$$\beta = \frac{a}{\sqrt{\frac{c_{11}}{\rho}}} \omega
 \tag{15}$$

variation of the determinants of the characteristic equation given in Eq. (14) with the dimensionless natural frequencies for different boundary conditions and aspect ratio of ($b/a=1.02$) is graphically illustrated in Fig. 2. As seen from the graphs, dimensionless natural frequencies make the determinant zero. There are various numerical methods to find the roots of Eq. (14).

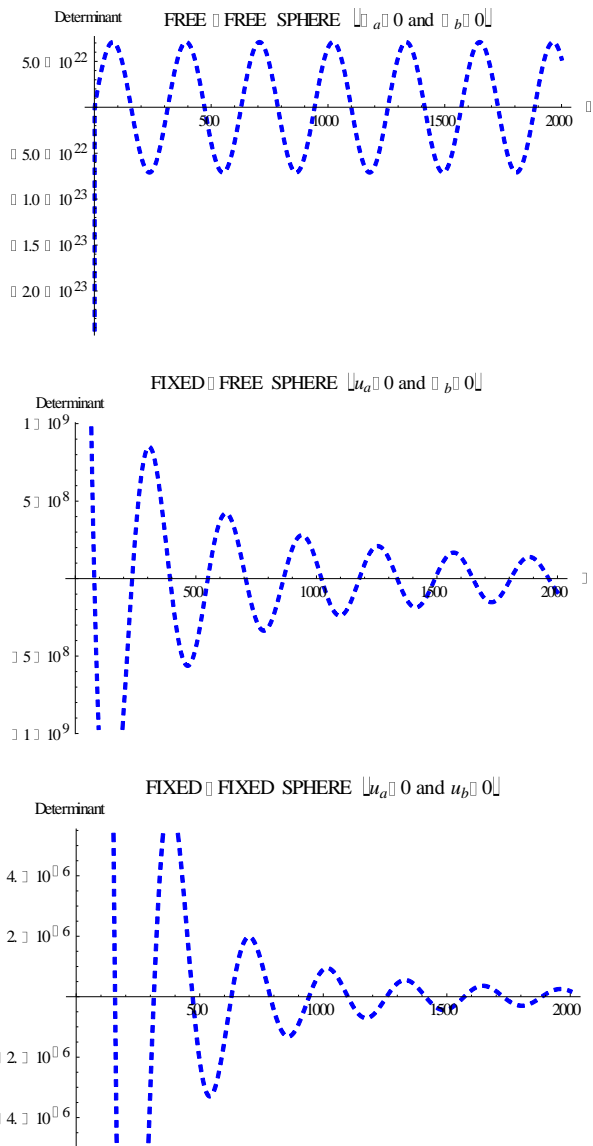


Fig. 2 Variation of the determinants of the characteristic equation given in (14) with the dimensionless natural frequencies for different boundary conditions and aspect ratio of ($b/a=1.02$).

3. Verification of the Results

The present dimensionless results obtained with Eq. (14) are compared with the literature for free-free ends and the aspect ratio of 2 in Table 2. A good agreement is observed between the results.

Table 2 Comparisons of the present natural frequencies with the literature for free-free ends, $\nu = 0.3$, and $b/a = 2$

β_i	Present	[36]	[37]
1	1.01034	1.01178	0.9781990865
2	3.33252	3.33527	3.296902510
3	6.37556	6.37694	6.358013920
4	9.48585	9.48676	9.474240635
5	12.612	12.61272	12.60335232
6	15.7444	15.74499	15.73750534
7	18.8799	18.88038	18.87415459
8	22.0172	22.01756	22.01222291
9	25.1555	25.15584	25.15117544
10	28.2946	28.29486	28.29071630

4. Variation of the Natural Frequencies with the Aspect Ratios and Boundary Conditions

Variation of the natural frequencies with the boundary conditions are presented for $\nu = 0.3$, and $b/a = 1.02$ in a comparative manner in Table 3. The first twelve dimensionless natural frequencies are given in this table.

Table 3 Variation of the natural frequencies with the boundary conditions for $b/a = 1.02$ and $\nu = 0.3$

β_i	Free-Free	Fixed-Free	Fixed-Fixed	Free-Fixed
1	1.4425	78.4629	157.086	78.6432
2	157.087	235.594	314.162	235.654
3	314.163	392.684	471.241	392.72
4	471.241	549.768	628.32	549.793
5	628.32	706.85	785.399	706.87
6	785.4	863.931	942.479	863.947
7	942.479	1021.01	1099.56	1021.03
8	1099.56	1178.09	1256.64	1178.1
9	1256.64	1335.17	1413.72	1335.18
10	1413.72	1492.25	1570.8	1492.26
11	1570.8	1649.33	1727.88	1649.34
12	1727.88	1806.41	1884.96	1806.42

As expected, Table 3 suggests that increasing the total number of the degrees of freedom at both ends decreases significantly the frequencies. This is the most noticeable characteristic among the fundamental frequencies. That is, while $\beta_1 = 1.4425$ for free-free ends, it reaches $\beta_1 = 157.086$ for fixed-fixed ends.

Variation of the first twelve natural frequencies with aspect ratios from $b/a = 1.03$ through $b/a = 2$ for all boundary conditions and $\nu = 0.3$ is presented in Table 4 in tabular form.

Table 4. Variation of the first twelve natural frequencies with aspect ratios and boundary conditions for $\nu = 0.3$

β_i	b/a									
	1.03	1.04	1.05	1.075	1.10	1.25	1.50	1.75	2.00	
FREE-FREE										
1	1.43546	1.42852	1.42167	1.4049	5	1.38876	1.30140	1.18376	1.08938	1.0103
2	104.73	78.5538	62.8492	41.913	3	31.449	12.6395	6.40647	4.34971	3.3325
3	209.445	157.087	125.672	83.788	5	62.8484	25.1692	12.6273	8.45626	6.3755
4	314.163	235.624	188.501	125.67	2	94.2588	37.7234	18.8901	12.6186	9.4858
5	418.882	314.163	251.332	167.55	8	125.672	50.2837	25.1631	16.7942	12.612
6	523.601	392.702	314.163	209.44	5	157.086	62.8464	31.4402	20.9752	15.744
7	628.32	471.241	376.994	251.33	2	188.501	75.4104	37.7193	25.1588	18.879
8	733.04	549.781	439.825	293.21	9	219.916	87.975	43.9996	29.3438	22.017
9	837.759	628.32	502.657	335.10	6	251.332	100.54	50.2806	33.5298	25.155
10	942.479	706.86	565.489	376.99	4	282.747	113.105	56.5621	37.7164	28.294
11	1047.2	785.4	628.32	418.88	2	314.163	125.671	62.844	41.9035	31.434
12	1151.92	863.939	691.152	460.76	9	345.578	138.237	69.1261	46.0909	34.574
FIXED-FIXED										
1	104.729	78.5521	62.847	41.910	1	31.4448	12.6294	6.38581	4.31683	3.2860
2	209.444	157.086	125.671	83.786	9	62.8463	25.1645	12.619	8.44465	6.3606
3	314.162	235.624	188.501	125.67	1	94.2574	37.7203	18.8848	12.6115	9.4772
4	418.881	314.162	251.331	167.55	7	125.671	50.2814	25.1592	16.7891	12.605
5	523.601	392.702	314.162	209.44	4	157.085	62.8446	31.4371	20.9712	15.739
6	628.32	471.241	376.994	251.33	1	188.5	75.4088	37.7168	25.1554	18.876
7	733.04	549.78	439.825	293.21	8	219.916	87.9737	43.9974	29.341	22.013
8	837.759	628.32	502.657	335.10	6	251.331	100.539	50.2787	33.5274	25.152
9	942.479	706.86	565.488	376.99	4	282.747	113.104	56.5605	37.7143	28.292
10	1047.2	785.399	628.32	418.88	1	314.162	125.67	62.8425	41.9015	31.431
11	1151.92	863.939	691.152	460.76	9	345.578	138.236	69.1247	46.0891	34.572
12	1256.64	942.479	753.983	502.65	7	376.994	150.802	75.4071	50.2768	37.712
FREE-FIXED										
1	52.4694	39.3855	31.5374	21.08	15.858	6.50815	3.46102	2.47932	2.0004	2

2	157.116	117.848	94.2882	62.877	47.1735	18.9226	9.52685	6.40655	4.8523
3	261.821	196.373	157.104	104.74	78.5696	31.4596	15.7688	10.5452	7.9366
4	366.535	274.906	219.929	146.62	109.977	44.0135	22.0345	14.7129	11.054
5	471.251	353.442	282.757	188.51	141.388	56.5729	28.3081	18.8901	14.182
6	575.969	431.979	345.586	230.39	172.801	69.1349	34.5851	23.0715	17.316
7	680.687	510.518	408.416	272.28	204.215	81.6982	40.864	27.2551	20.451
8	785.405	589.056	471.247	314.16	235.629	94.2623	47.1441	31.4402	23.589
9	890.124	667.595	534.078	356.05	267.044	106.827	53.4249	35.6261	26.727
10	994.843	746.134	596.909	397.94	298.459	119.392	59.7062	39.8127	29.866
11	1099.56	824.674	659.74	439.82	329.874	131.957	65.9879	43.9996	33.006
12	1204.28	903.213	722.572	481.71	361.29	144.523	72.2698	48.1869	36.146
FIXED-FREE									
1	52.2898	39.2064	31.3589	20.902	15.6807	6.32563	3.25556	2.24722	1.7444
2	157.056	117.789	94.229	62.818	47.1155	18.8673	9.4737	6.3535	4.7978
3	261.785	196.337	157.068	104.71	78.5348	31.4267	15.7379	10.5154	7.9073
4	366.509	274.88	219.903	146.60	109.952	43.9901	22.0127	14.692	11.034
5	471.231	353.422	282.737	188.49	141.369	56.5547	28.2911	18.874	14.167
6	575.952	431.963	345.57	230.38	172.785	69.12	34.5713	23.0584	17.303
7	680.673	510.504	408.403	272.26	204.202	81.6856	40.8523	27.2441	20.441
8	785.394	589.044	471.235	314.15	235.618	94.2514	47.134	31.4306	23.580
9	890.114	667.585	534.067	356.04	267.034	106.817	53.416	35.6177	26.719
10	994.834	746.125	596.90	397.93	298.45	119.383	59.6982	39.8051	29.859
11	1099.55	824.665	659.732	439.82	329.866	131.949	65.9807	43.9928	32.999
12	1204.27	903.205	722.564	481.70	361.282	144.516	72.2632	48.1807	36.140

Variation of the first six natural frequencies of free-free sphere is also illustrated graphically in Figs. 3-5.

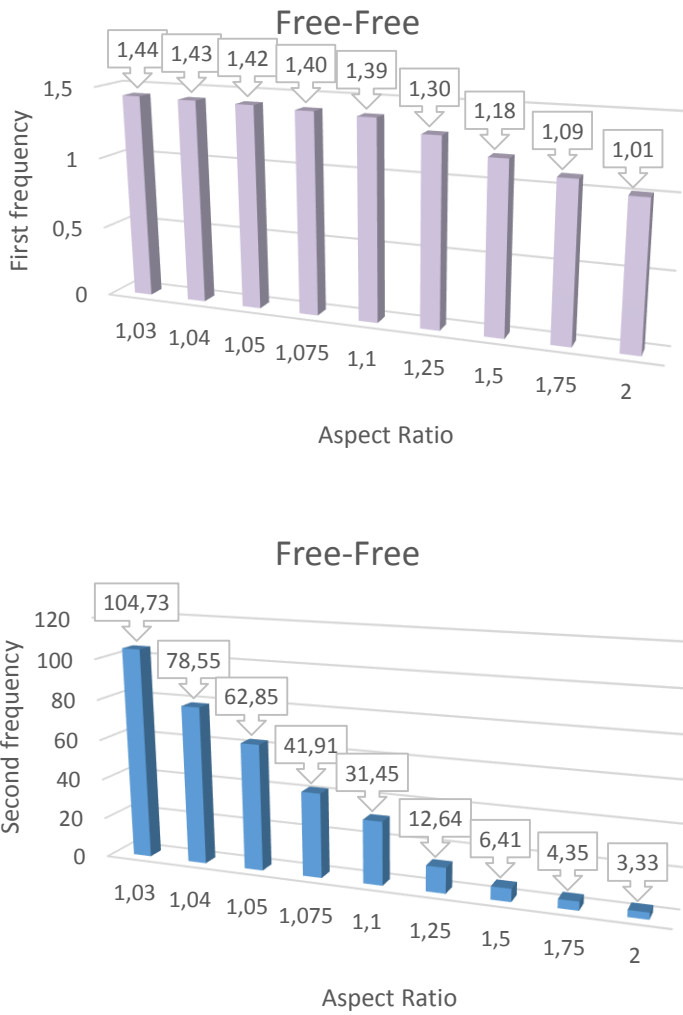


Fig. 3 Variation of the first and second natural frequencies of the sphere with the aspect ratios ($\nu = 0.3$)

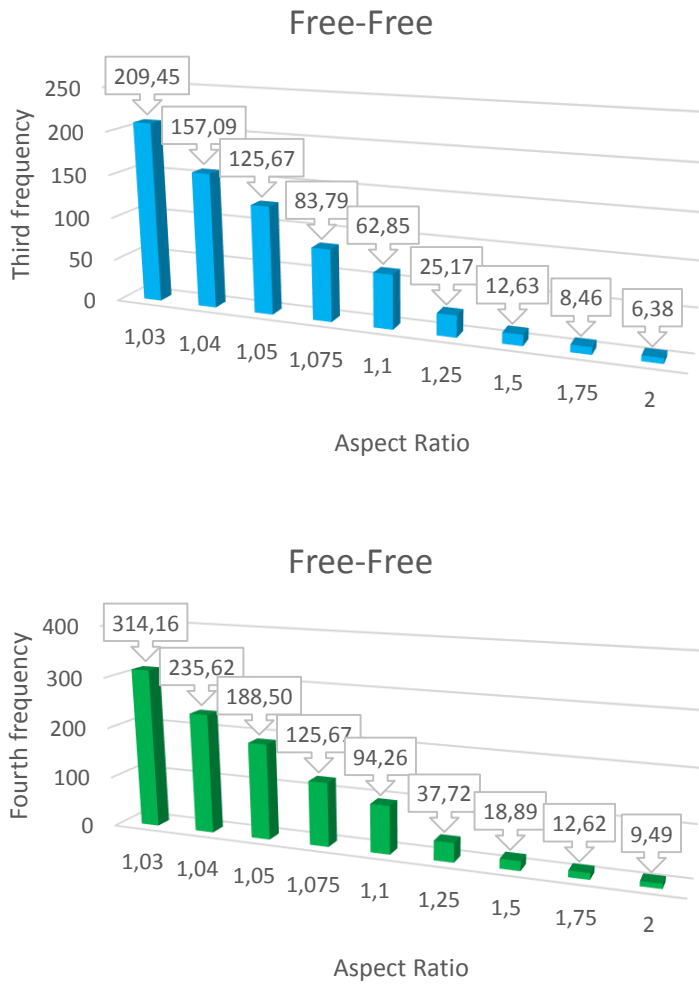


Fig. 4 Variation of the third and fourth natural frequencies of the sphere with the aspect ratios ($\nu = 0.3$)



Fig. 5 Variation of the fifth and sixth natural frequencies of the sphere with the aspect ratios. ($\nu = 0.3$)

From Table 4 and Figs. 3 and 4, it is seen that when the thickness of the sphere increases, the dimensionless natural frequencies become smaller. Higher dimensionless natural frequencies are observed for thin-walled spheres. There are minor differences in frequencies under fixed-free and free-fixed boundary conditions. Natural frequencies of the sphere with fixed-free surfaces are slightly lesser than the one with free-fixed boundaries.

5. Case Study

Today's works have focused on research to further improve composite material properties. Metal-matrix composites (MMCs) is a group of advanced materials. The interest in carbon nanotubes (CNTs) as reinforcements for aluminium (Al) has been growing considerably. Neubauer et al. [41] presented an overview and summarized the activities related to carbon nanotubes and nanofibers used as a reinforcement in metallic matrix materials. They also discussed the main challenges and the potential with respect to material properties.

In this section, a case study with a hollow sphere made of a metal-matrix composite is to be originally conducted to show the direct application of the present results. The composite material is formed by the perfect uniform dispersion of carbon nanotubes (CNTs) into Aluminium (Al) metal matrix. Two types of CNTs are considered, namely single-walled carbon-nanotubes (SWCNT) and multi-walled carbon-nanotubes (MWCNT). To get a homogeneous and isotropic composite material, up to 5 wt.%CNT is dispersed in Al matrix. Otherwise, the resulting composite is to show anisotropic material characteristics. CNT properties have been taken from Costa et al.'s study [48]: Material properties of a metallic matrix are

$$E_m = E_{Al} = 70 \text{ GPa}, \quad \nu_m = \nu_{Al} = 0.3, \quad \rho_m = \rho_{Al} = 2700 \text{ k/m}^3$$

Material and geometrical properties of SWCNTs are [48]

$$E_{SWCNT} = 640 \text{ GPa}, \quad \nu_{SWCNT} = 0.33, \quad \rho_{SWCNT} = 1350 \text{ k/m}^3$$

$$l_{SWCNT} = 25 (\mu\text{m}), \quad d_{SWCNT} = 1.4(\text{nm}), \quad t_{SWCNT} = 0.34(\text{nm})$$

Material and geometrical properties of MWCNTs are [48]

$$E_{MWCNT} = 400 \text{ GPa}, \quad \nu_{MWCNT} = 0.33, \quad \rho_{MWCNT} = 1350 \text{ k/m}^3$$

$$l_{MWCNT} = 50 (\mu\text{m}), \quad d_{MWCNT} = 20(\text{nm}), \quad t_{MWCNT} = 0.34(\text{nm})$$

In the above d , t , and l are the diameter, thickness, and length of a CNT, respectively. Poisson's ratio and the density of the resulting composite are computed by using a simple mixture rule as follows

where V_{CNT} denotes the volume fraction of CNTs and it is calculated by using CNTs weight fraction, w_{CNT} .

$$V_{CNT} = \frac{w_{CNT}}{w_{CNT} + \left(\frac{\rho_{CNT}}{\rho_m}\right) - \left(\frac{\rho_{CNT}}{\rho_m}\right)w_{CNT}} \quad (17)$$

It may be noted that both the length efficiency and the orientation efficiency factors are taken as unit in Eq. (16) due to the present assumptions. Young's modulus of the composite is to be estimated through Halpin-Tsai equations [48-49].

$$E_{m-CNT} = \frac{E_m}{8} \left(5 \left(\frac{1 + 2\beta_{dd}V_{CNT}}{1 - \beta_{dd}V_{CNT}} \right) + 3 \left(\frac{1 + 2 \left(\frac{l_{CNT}}{d_{CNT}} \right) \beta_{dl}V_{CNT}}{1 - \beta_{dl}V_{CNT}} \right) \right) \quad (18)$$

where

$$\beta_{dl} = \frac{\left(\frac{E_{CNT}}{E_m}\right) - \left(\frac{d_{CNT}}{4t_{CNT}}\right)}{\left(\frac{E_{CNT}}{E_m}\right) + \left(\frac{l_{CNT}}{2t_{CNT}}\right)}, \quad \beta_{dd} = \frac{\left(\frac{E_{CNT}}{E_m}\right) - \left(\frac{d_{CNT}}{4t_{CNT}}\right)}{\left(\frac{E_{CNT}}{E_m}\right) + \left(\frac{d_{CNT}}{2t_{CNT}}\right)} \quad (19)$$

Variation of the effective properties of the composite with CNTs weight fraction up to 5 wt.%CNT is seen in Fig. 6. As can be seen from the figure that Poisson’s ratio of the composite formed either SWCNT or MWCNT increase with increasing weight fraction while the density of the composite decrease with increasing weight fraction. It is revealed that both SWCNT and MWCNT make the same difference in values of Poisson’s ratio and the density. However, there is a significant difference in the values of Young’s modulus. When SWCNTs enhance elasticity modulus of the composite with increasing weight fractions, MWCNTs make the opposite.

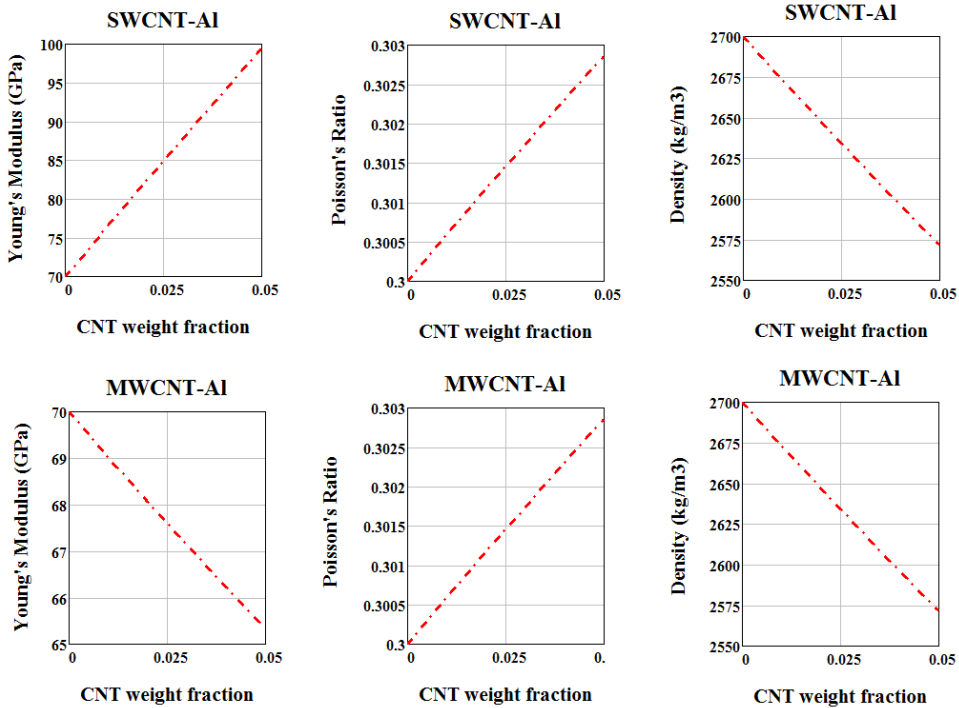


Fig. 6 Variation of the effective properties of the composite with CNTs weight fraction

In the present study three numerical values of CNTs weight fraction are chosen. Material properties of the resulting composite are tabulated in Table 5 with respect to the chosen CNTs weight fraction values.

Table 5. Material properties of the resulting composite

w_{SWCNT}	$E_{m-SWCNT}$ (GPa)	$\nu_{m-SWCNT}$	$\rho_{m-SWCNT}$ (kg/m ³)
0.0	70.0	0.3	2700
0.01	76.01	0.301	2673
0.025	84.9	0.301	2634
0.05	99.42	0.303	2571
w_{MWCNT}	$E_{m-MWCNT}$ (GPa)	$\nu_{m-MWCNT}$	$\rho_{m-MWCNT}$ (kg/m ³)
0.0	70.0	0.3	2700
0.01	69.02	0.301	2673
0.025	67.60	0.301	2634
0.05	65.35	0.303	2571

Let's write the dimensionless natural frequency in Eq. (15) in a more explicit form as follows

$$\beta = \frac{a}{\sqrt{\frac{c_{11}}{\rho}}} \omega = \frac{a}{\sqrt{\frac{\lambda+2\mu}{\rho}}} \omega = \frac{a}{\sqrt{\frac{E(1-\nu)}{\rho(1+\nu)(1-2\nu)}}} \omega \tag{20}$$

The relationship between the natural frequencies and the ratio of (β/a) are presented in Table 6. Table 6 also comprises the percentage relative increase/decrease compared to a sphere made of a pure aluminum.

Table 6. Natural frequencies in terms of (β/a)

w_{SWCNT}	ω (rad/s)	ω (kHz)	$\left \frac{\omega_m - \omega_{m-SWCNT}}{\omega_m} \right 100$
0.0	5907.646308(β/a)	0.940231(β/a)	0
0.01	6191.731479(β/a)	0.985445(β/a)	4.81
0.025	6600.404350(β/a)	1.050487(β/a)	11.73
0.05	7243.810673(β/a)	1.152888(β/a)	22.62
w_{MWCNT}	ω (rad/s)	ω (kHz)	$\left \frac{\omega_m - \omega_{m-MWCNT}}{\omega_m} \right 100$
0.0	5907.646308(β/a)	0.939067(β/a)	0
0.01	5900.334574(β/a)	0.937371(β/a)	0.12
0.025	5889.673752(β/a)	0.934663(β/a)	0.30
0.05	5872.658190(β/a)	0.939067(β/a)	0.59

It can be seen from Table 6 that 1wt.%SWCNT dispersion escalates the natural frequencies by approximately 5%, 2.5wt.%SWCNT dispersion makes an increase approximately 12%, and 5 wt.%SWCNT dispersion buildups the frequencies by approximately 23%. MWCNT dispersion into Al matrix makes almost no significant differences in natural frequencies. In other words, approximately the same natural frequencies may be obtained by dispersing MWCNT into Al matrix by obtaining 5% lighter material. SWCNT inclusion into Al matrix affects both the weight of the material and natural frequencies. In the design and optimization of the structures, it is requested to have larger natural frequencies for the same weight of structure.

As a numerical example let's consider a hollow sphere made of either a steel or an aluminium. For this materials, the wave velocity having been a wave property may be computed numerically as

$$\left(\sqrt{\frac{\lambda + 2\mu}{\rho}}\right)_{Steel} = 5875.097045 \text{ m/s } (E = 200GPa, \rho = 7800 \text{ kg/m}^3, \nu = 0.3)$$

$$\left(\sqrt{\frac{\lambda + 2\mu}{\rho}}\right)_{Aluminium} = 5907.646308 \text{ m/s } (E = 70GPa, \rho = 2700 \text{ kg/m}^3, \nu = 0.3)$$

From Eq. (20) the following is obtained for the natural frequency in kHz.

$$\omega = \sqrt{\frac{\lambda + 2\mu}{\rho}} \frac{(\beta/a)}{2\pi} \frac{1}{1000} \text{ (kHz)}$$

Let's assume $a = 1\text{cm}$ and $b = 2\text{cm}$. For the ratio of $b/a = 2$ and for a sphere under free-free boundary conditions, the dimensionless fundamental natural frequency is read as $\beta = 1.01034$ from Table 4. The dimensional natural frequency is, accordingly, found as

$$\omega_{Steel} = (5875.097045) \frac{(1.01034)}{(0.01)} \frac{1}{2\pi} \frac{1}{1000} = 94.47 \text{ kHz}$$

$$\omega_{Aluminium} = (5907.646308) \frac{(1.01034)}{(0.01)} \frac{1}{2\pi} \frac{1}{1000} = 94.995 \text{ kHz}$$

As a final example, let's consider Kim et al.'s example sphere under free-free surfaces [50]: $E = 53.2GPa, \rho = 7700 \text{ kg/m}^3, \nu = 0.261, b/a = 10\text{mm}/8\text{mm} = 1.25$. Since Table 4 has been prepared for $\nu = 0.3$, the dimensionless fundamental frequency needs to be recalculated by using Eq. (14a). Yıldırım [38] has given this value as $\beta = 1.32553$. By using this data, the following results are obtained:

$$\sqrt{\frac{\lambda + 2\mu}{\rho}} = 2910.456959 \text{ m/s}$$

$$\omega_{Present} = (2910.456959) \frac{(1.32553)}{(0.008)} \frac{1}{2\pi} \frac{1}{1000} = 76.75044234 \text{ kHz}$$

This results overlaps with the open literature:

$$\omega_{Kim \text{ et al.}[50]} = 76.7 \text{ kHz}$$

$$\omega_{Yıldırım [38]} = 76.75044 \text{ kHz}$$

6. Conclusions

In this work the exact one-dimensional axisymmetric radial free vibration analysis of a thick-walled sphere was handled systematically. Frequency equations in terms of spherical Bessel functions were presented in closed form for four possible classical boundary conditions. The numerical results were verified with the available literature.

Besides, a parametric study for the investigation of natural frequencies with both the sphere aspect ratios and boundary conditions was conducted for the isotropic and homogeneous linear elastic materials having Poisson ratio of $\nu = 0.3$. The following distinctive features were observed:

- i. Increasing the total number of the degrees of freedom at both ends decreases significantly the frequencies. This is the most noticeable characteristic among the fundamental frequencies. As a consequence of this, free-free ends offer the smallest natural frequency. The converse is true for fixed-fixed ends.
- ii. There is no such a significant difference between the natural frequencies of fixed-free and free-fixed boundary conditions for $1.02 \leq b/a \leq 2$ and $\nu = 0.3$. Those differences, however, become more obvious towards $b/a = 2$.
- iii. An increase in the thickness of the sphere makes the dimensionless natural frequencies small. Thin-walled spheres have higher dimensionless natural frequencies than thick-walled ones.

Since the interest in CNT-reinforced aluminum composites has been growing considerably, a case study with an aluminum matrix dispersed by either SWCNT or MWCNT was carried out. Enhancements of up to 23% in natural frequencies compared to pure aluminium were observed for the inclusion of 5 wt.%SWCNT into *Al* matrix. It was also revealed that MWCNT inclusion into *Al* matrix makes almost does not a contribution on the natural frequencies.

In conclusion, it was seen that the given closed-form characteristic equations and some numerical results in the present work may readily be used for hollow spheres made of any kind of isotropic and homogeneous linear elastic material even for some kind of CNT reinforced composites.

Acknowledgement: I thank to the referees for the effort and time spent together with their constructive feedback.

References

- [1] Horace Lamb MA. On the vibrations of an elastic sphere. Proceedings of the London Mathematical Society, 1881; 1-13 (1): 189–212.
- [2] Horace Lamb MA. On the vibrations of a spherical shell. Proceedings of the London Mathematical Society, 1882; 14(1): 50-56. <https://doi.org/10.1112/plms/s1-14.1.50>
- [3] Sato Y, Usami T. Basic study on the oscillation of homogeneous elastic sphere-part I. Frequency of the free oscillations. Geophysics Magazine, 1962; 31(1): 15-24.
- [4] Sato, Y, Usami T. Basic study on the oscillation of homogeneous elastics sphere-part II. Distribution of displacement", Geophysics Magazine, 1962; 31(1): 25-47.
- [5] Shah H, Ramkrishana CV, Datta SK. Three dimensional and shell theory analysis of elastic waves in a hollow sphere-part I. Analytical foundation. ASME, Journal of Applied Mechanics, 1969; 36(3): 431-439. <https://doi.org/10.1115/1.3564698>
- [6] Shah H, Ramkrishana CV, Datta SK. Three dimensional and shell theory analysis of elastic waves in a hollow sphere-part II. Numerical results. ASME, Journal of Applied Mechanics, 1969; 36(3): 440-444. <https://doi.org/10.1115/1.3564699>
- [7] Seide P. Radial vibrations of spherical shells. J. Appl. Mech, 1970; 37(2): 528-530. <https://doi.org/10.1115/1.3408540>
- [8] Scaffbuch PJ, Rizzo FJ, Thomson RB. Eigen frequencies of an elastic sphere with fixed boundary conditions. J. Appl. Mech., 1992; 59(2): 458–459. <https://doi.org/10.1115/1.2899545>
- [9] Gosh AK, Agrawal MK. Radial vibrations of spheres. Journal of Sound and Vibration, 1994; 171(3): 315–322. <https://doi.org/10.1006/jsvi.1994.1123>

- [10] Abbas I. Analytical solution for a free vibration of a thermoelastic hollow sphere. *Mechanics Based Design of Structures and Machines*, 2015; 43(3): 265-276. <https://doi.org/10.1080/15397734.2014.956244>
- [11] Sharma JN, Sharma N. Free vibration analysis of homogeneous thermoelastic solid sphere. *Journal of Applied Mechanics, ASME*, 2010; 77(2): 021004. <https://doi.org/10.1115/1.3172141>
- [12] Sharma N. Modeling and analysis of free vibrations in thermoelastic hollow spheres. *Multidiscipline modeling in materials and structures*, 2015; 11(2): 134-159. <https://doi.org/10.1108/MMMS-05-2014-0033>
- [13] Hoppmann II WH, Baker WE. Extensional vibrations of elastic orthotropic spherical shells. *Journal of Applied Mechanics*, 1961; 28: 229-237. <https://doi.org/10.1115/1.3641659>
- [14] Eason G. On the vibration of anisotropic cylinders and spheres. *Applied Scientific Research, Section A*, 1963; 12: 81-85. <https://doi.org/10.1007/BF03184751>
- [15] Cohen H, Shah AH. Free vibrations of a spherically isotropic hollow sphere. *Acustica*, 1972; 26: 329-333.
- [16] Nelson RB. Natural vibrations of laminated orthotropic spheres. *International Journal of Solids and Structures*, 1973; 9(3): 305-311. [https://doi.org/10.1016/0020-7683\(73\)90081-4](https://doi.org/10.1016/0020-7683(73)90081-4)
- [17] Shul'ga NA, Grigorenko AY, E'mova TL. Free non-axisymmetric oscillations of a thick-walled, nonhomogeneous, transversely isotropic, hollow sphere. *Soviet Applied Mechanics*, 1988; 24: 439-444. <https://doi.org/10.1007/BF00883063>
- [18] Grigorenko YM, Kilina TN. Analysis of the frequencies and modes of natural vibration of laminated hollow spheres in three-dimensional and two-dimensional formulations. *Soviet Applied Mechanics*, 1989; 25: 1165-1171. <https://doi.org/10.1007/BF00887140>
- [19] Heyliger PR, Jilani A. The free vibrations of inhomogeneous elastic cylinders and spheres. *International Journal of Solids and Structures*, 1992; 29(22): 2689-2708. [https://doi.org/10.1016/0020-7683\(92\)90112-7](https://doi.org/10.1016/0020-7683(92)90112-7)
- [20] Jiang H, Young PG, Dickinson SM. Natural frequencies of vibration of layered hollow spheres using three-dimensional elasticity equations. *Journal of Sound and Vibration*, 1996; 195(1): 155-162. <https://doi.org/10.1006/jsvi.1996.0412>
- [21] Ding HJ, Chen WQ. Nonaxisymmetric free vibrations of a spherically isotropic spherical shell embedded in an elastic medium. *International Journal of Solids and Structures*, 1996; 33: 2575-2590. [https://doi.org/10.1016/0020-7683\(95\)00171-9](https://doi.org/10.1016/0020-7683(95)00171-9)
- [22] Ding HJ, Chen WQ. Natural frequencies of an elastic spherically isotropic hollow sphere submerged in a compressible fluid medium. *Journal of Sound and Vibration*, 1996; 192(1): 173-198. <https://doi.org/10.1006/jsvi.1996.0182>
- [23] Chen WQ, Ding HJ. Natural frequencies of a fluid-filled anisotropic spherical shell. *Journal of the Acoustical Society of America*, 1999; 105: 174-182. <https://doi.org/10.1121/1.424578>
- [24] Chen WQ, Cai JB, Ye GR, Ding HJ. On eigen frequencies of an anisotropic sphere. *ASME, Journal of Applied Mechanics*, 2000; 67(2): 422-424. <https://doi.org/10.1115/1.1303803>
- [25] Chen WQ, Ding HJ. Free vibration of multi-layered spherically isotropic hollow spheres. *International Journal of Mechanical Sciences*, 2001; 43(3): 667-680. [https://doi.org/10.1016/S0020-7403\(00\)00044-8](https://doi.org/10.1016/S0020-7403(00)00044-8)
- [26] Stavsky Y, Greenberg JB. Radial vibrations of orthotropic laminated hollow spheres. *J Acoust Soc Am*, 2003; 113: 847-851. <https://doi.org/10.1121/1.1536625>
- [27] Ding HJ, Wang HM. Discussions on "Radial vibrations of orthotropic laminated hollow spheres" [*J Acoust Soc Am*, 113, 847-851 (2003)]. *The Journal of the Acoustical Society of America*, 2004; 115: 1414. <https://doi.org/10.1121/1.1649911>
- [28] Sharma JN, Sharma N. Vibration analysis of homogeneous transversely isotropic generalized thermoelastic spheres. *Journal of Vibration and Acoustics, ASME*, 2011; 133(4): 041001. <https://doi.org/10.1115/1.4003396>

- [29] Keles İ. Novel approach to forced vibration behavior of anisotropic thick-walled spheres. AIAA Journal, 2016; 54(4): 1438-1442. <https://doi.org/10.2514/1.J054322>
- [30] Chen WQ, Ding HJ, Xu RQ. Three-dimensional free vibration analysis of a fluid-filled piezoceramic hollow sphere. Computers and Structures, 2001; 79(6): 653-663. [https://doi.org/10.1016/S0045-7949\(00\)00166-8](https://doi.org/10.1016/S0045-7949(00)00166-8)
- [31] Chiroiu V, Munteanu L. On the free vibrations of a piezoceramic hollow sphere. Mechanics Research Communications, 2007; 34: 123-129. <https://doi.org/10.1016/j.mechrescom.2006.06.011>
- [32] Chen WQ, Wang X, Ding, HJ. Free vibration of a fluid-filled hollow sphere of a functionally graded material with spherical isotropy. Journal of the Acoustical Society of America, 1999; 106: 2588-2594. <https://doi.org/10.1121/1.428090>
- [33] Chen WQ, Wang LZ, Lu Y. Free vibrations of functionally graded piezoceramic hollow spheres with radial polarization. Journal of Sound and Vibration, 2002; 251(1): 103-114. <https://doi.org/10.1006/jsvi.2001.3973>
- [34] Ding HJ, Wang HM, Chen WQ. Dynamic responses of a functionally graded pyroelectric hollow sphere for spherically symmetric problems. Int J Mech Sci, 2003; 45: 1029-1051. <https://doi.org/10.1016/j.ijmecsci.2003.09.005>
- [35] Kanoria M, Ghosh MK. Study of dynamic response in a functionally graded spherically isotropic hollow sphere with temperature dependent elastic parameters. J Thermal Stresses, 2010; 33: 459-484. <https://doi.org/10.1080/01495731003738440>
- [36] Keleş İ, Tütüncü N. Exact analysis of axisymmetric dynamic response of functionally graded cylinders (or disks) and spheres. Journal of Applied Mechanics; 78 (6), 061014, 2011 (7 pages).
- [37] Sharma PK, Mishra, KC. Analysis of thermoelastic response in functionally graded hollow sphere without load. Journal of Thermal Stresses, 2017; 40(2), 185-197. <https://doi.org/10.1080/01495739.2016.1231024>
- [38] Yıldırım, V. Exact radial free vibration frequencies of power-law graded spheres. Journal of Applied and Computational Mechanics, 2018; 4(3): 175-186. doi: [10.22055/JACM.2017.22987.1145](https://doi.org/10.22055/JACM.2017.22987.1145)
- [39] Esawi AMK, Morsi K, Sayed A, Abdel Gawad A, Borah P. Fabrication and properties of dispersed carbon nanotube-aluminium composites. Mater Sci Eng A, 2009; 508(1-2): 167-173. <https://doi.org/10.1016/j.msea.2009.01.002>
- [40] Esawi AMK, Morsi K, Sayed A, Taher M, Lanka S. Effect of carbon nanotube (CNT) content on the mechanical properties of CNT-reinforced aluminium composites. Composites Science and Technology, 2010; 70(16): 2237-2241. <https://doi.org/10.1016/j.compscitech.2010.05.004>
- [41] Neubauer E, Kitzmantel M, Hulman M, Angerer P. Potential and challenges of metal-matrix-composites reinforced with carbon nanofibers and carbon nanotubes. Composites Science and Technology, 2010; 70: 2228-2236. <https://doi.org/10.1016/j.compscitech.2010.09.003>
- [42] Yıldırım, V. Exact radial natural frequencies of functionally graded hollow long cylinders. International Journal of Engineering & Applied Sciences (IJEAS), 2017; 9(4): 28-41. <https://doi.org/10.24107/ijeas.336621>
- [43] Yıldırım, V. Exact in-plane natural frequencies in purely radial modes and corresponding critical speeds of functionally graded (FG) non-uniform disks, American Journal of Modern Physics and Application, 2018; 5(1): 9-23.
- [44] Watson GN. A Treatise on the Theory of Bessel Functions. Cambridge University Press, 1922.
- [45] Bowman F. Introduction to Bessel functions, New York: Dover, 1958.
- [46] Hildebrand FB. Advanced Calculus for Applications. Prentice-Hall, Inc. Englewood Cliffs, New Jersey, 1962.
- [47] Abramowitz M, Stegun, IA (Eds.). §9.1.1 in Handbook of Mathematical Functions with Formulas, Graphs, and Mathematical Tables, 9th printing, New York, Dover, 1972.

- [48] Costa DMS, Loja MAR. On the characterization of the free vibrations behavior of multiscale composite plates. *Research on Engineering Structures and Materials (RESM)*, 2017; 3(1): 27-44. <https://doi.org/10.17515/resm2016.43st0602>
- [49] Halpin, JC, Kardos, JL. The Halpin-Tsai Equations: A Review. *Polymer Engineering and Science*, 1976; 344:352, 16(5).
- [50] Kim JO, Lee JG, Chun HY. Radial vibration characteristics of spherical piezoelectric transducers, *Ultrasonics*, 2005; 43: 531–537. <https://doi.org/10.1016/j.ultras.2005.01.004>